

Rotational correlation functions and apparently enhanced translational diffusion in a free-energy landscape model for the α relaxation in glass-forming liquids

Gregor Diezemann, Hans Sillescu, Gerald Hinze and Roland Böhmer

Institut für Physikalische Chemie, Johannes Gutenberg-Universität Mainz, 55099 Mainz, Federal Republic of Germany

(Received 7 July 1997; revised manuscript received 1 December 1997)

We explore a simple model for supercooled liquids in which reorientational and translational motions are inherently coupled to the structural relaxation. Several controversial aspects of the molecular motion in glass-forming materials are naturally resolved within the framework of our model. These include the geometry of the molecular reorientations as well as the apparent enhancement of translational diffusion. The breakdown of the Stokes-Einstein relation is thus explained without assuming the existence of local diffusion coefficients.

[S1063-651X(98)04404-3]

PACS number(s): 64.70.Pf

I. INTRODUCTION

In a recent paper [1], denoted as I in the following, a free-energy landscape model was introduced in which the rotational molecular motion is associated with transitions between different dynamical (nonergodic, metastable) states, i.e., with structural relaxation. In particular, it was assumed that molecular reorientation is completely determined by the rates $\kappa(\epsilon, \epsilon')$ of transitions $\epsilon' \rightarrow \epsilon$ connecting states ϵ on a free-energy hypersurface. This obviates the necessity of having to introduce the time scale for the reorientations separately. In other words, any transition from a molecular orientation Ω to a different orientation Ω' is associated with a corresponding transition among the states ϵ , which defines the minima in the free-energy landscape. The model starts from a composite Markov process [2] $[\epsilon(t), \Omega(t)]$ from which the non-Markovian process of molecular reorientation, $\Omega(t)$, is obtained as a projection from the composite process by integrating over all states ϵ . The consequences of this model for the evaluation of higher order correlation functions were dealt with in I and then used to analyze recent reduced four-dimensional NMR experiments [3–5]. However, it was also shown how the model can be applied to other experiments in which a selected subensemble is monitored during its return to the dynamics of the full ensemble, such as, e.g., nonresonant dielectric hole burning [6].

In the present paper, we apply the model to various other aspects of α relaxation in supercooled liquids. A large number of different experimental observations have been accumulated in the past decades that document a very rich and complex phenomenology of the α relaxation. No *ab initio* theory is available for describing the dynamics of supercooled liquids close to the caloric glass transition temperature T_g . Therefore it is not surprising that vastly different theoretical concepts have been developed in order to give a *phenomenological* description. One such approach is the energy landscape model, which has extensively been studied in the past [7–12] in various formulations (see Ref. [13] for a recent discussion of the potential energy landscape picture). The particular version presented in this paper aims at a quantitative (or at least semiquantitative) description of a maximum number of experimental observations with a minimum

number of adjustable parameters.

One issue that we will address in detail is the nonexponentiality of the response functions measured in supercooled liquids. In comparing the results of relaxation functions obtained in different experiments there is often a notable degree of agreement, suggesting that these functions are dominated by the same or at least closely related molecular mechanisms. Thus, it was observed that not only dielectric relaxation [14] but also relaxation of poled mesogenic sidegroups in polymers [15] occurs on the same time scale as enthalpy relaxation. Furthermore in dynamic light scattering experiments it has been found that the time scales for molecular reorientation and density fluctuations detected in VH and VV scattering geometry [16] are similar.

It will be discussed further below that this agreement can be understood within the free-energy landscape model. It will also explain certain differences in the degree of nonexponentiality expressed, say, by the stretching parameter β_K of the Kohlrausch function $\exp[-(t/\tau)^{\beta_K}]$ when considering correlation functions obtained by different experimental techniques [17].

The mean rotational correlation times $\langle \tau_l \rangle$ where l denotes the rank of the Legendre polynomial (e.g., $l=1$ for dielectric relaxation, $l=2$ for NMR or light scattering) were found to be nearly independent of the rank l in supercooled liquids close to T_g , in particular $\langle \tau_1 \rangle \approx \langle \tau_2 \rangle$. This fact was interpreted as evidence for molecular reorientation by large-angle jumps, i.e., taken to rule out small-angle rotational diffusion [18–20]. This conclusion was challenged by Spiess during a general discussion on “viscous liquids and the glass transition” [21] where he argued that it should be difficult to determine the difference between $\langle \tau_1 \rangle$ and $\langle \tau_2 \rangle$, which often amounts to a relative shift of a few percent within distributions having a width of some decades [22]. He mentioned that from two-dimensional (2D) NMR studies on polymeric glass formers it has to be concluded that reorientations occur by small angular steps. In this discussion, Williams [23] argued on the basis of results from dielectric relaxation and Kerr effect studies that the quality of the data obtained in his group was sufficient in order to rule out the small angular step model. He rather favored the large angular (random) jump model for the description of reorientations in super-

cooled liquids like *o*-terphenyl (see also the literature quoted in [24]). As will be shown below (see Fig. 3) the present model provides an explanation of why $\langle \tau_1 \rangle \approx \langle \tau_2 \rangle$ can be found in experiments although reorientation proceeds in small angular steps [25]. The occurrence of small angle processes was also inferred from $^2\text{H-NMR}$ stimulated echo experiments in several supercooled liquids such as *o*-terphenyl, toluene, and glycerol [26–29].

Another example of an experimental finding that has led to controversial discussions is the enhancement of translational diffusion in comparison with shear viscosity and rotational diffusion on approaching the glass transition [30–33]. In the present model the apparent enhancement is seen to arise from taking different averages over the transition rates. An important feature of our approach is that we arrive at this result *without* assuming the Stokes-Einstein and Debye relations to hold locally.

Finally, some comments on the use of a free-energy landscape model are in order. We mention that the notion of free-energy minima inherently implies a coarse graining with respect to the density of the liquid over a certain spatial extent. Neither the magnitude nor the temperature dependence of a length scale associated with this coarse graining are known at present. Consequently, we will not attempt to give any estimates of the spatial extension of domains or regions in supercooled liquids.

The paper is organized as follows. In the next section we present the model used for the description of reorientational and translational motions in supercooled liquids. We then discuss the question of the impact of different angular jump models on experimental observables in Sec. III. Section IV is devoted to the application of the model to the translational diffusion of molecules and a discussion of the enhancement of these as compared to rotations. After a discussion of our results in Sec. IV we close with some conclusions.

II. ACTIVATED DYNAMICS MODEL FOR ROTATIONAL AND TRANSLATIONAL MOTION IN SUPERCOOLED LIQUIDS

In this section we briefly recall the main ingredients of the model for molecular reorientations in glass-forming liquids proposed earlier in [1] and show how rotations and translational diffusion can be treated on the same footing.

There are indications, e.g., from the mode coupling approach to the structural glass transition [34] and from computer simulations [35,36] of a thermally activated nature of α relaxation below a crossover temperature T_c located in the moderately supercooled regime. This point of view has already been advocated by Goldstein almost 30 years ago [7]. Explicit calculations based on a master equation approach [8–11] have shown the ability of such an approach to account for many aspects of the phenomenology of the α relaxation, such as the deviations from an Arrhenius law for the mean relaxation times or the stretching of the enthalpy relaxation functions.

Some models for the structural glass transition [12,37,38] seem to provide evidence for the existence of a large number of nonergodic states corresponding to different minima in the free-energy landscape in the supercooled liquid regime below a dynamic crossover temperature. (Whether this tem-

perature coincides with the mode coupling critical temperature T_c is still an open question.) These states are viewed as metastable since the free-energy barriers separating them do not appear to be macroscopic. Thermally activated dynamics proceeding via transitions in the free energy landscape thus restores ergodicity.

In view of the lack of understanding of the mechanism of the activated processes in supercooled liquids, we utilize an approach that is similar to the one adopted by Brawer [8], Dyre [9], and Bässler [10]. To each of the many minima in the free-energy landscape we assign a metastable (glass) state labeled by a single variable ϵ . A density of states (DOS), $\eta(\epsilon)$, is used to account for the total number of minima between ϵ and $\epsilon + d\epsilon$. The α relaxation is then modeled using a master equation [2], which reads

$$\begin{aligned} \dot{G}(\epsilon, \epsilon_0, t) = & - \int d\epsilon' \kappa(\epsilon', \epsilon) G(\epsilon, \epsilon_0, t) \\ & + \int d\epsilon' \kappa(\epsilon, \epsilon') G(\epsilon', \epsilon_0, t). \end{aligned} \quad (1)$$

Here, $G(\epsilon, \epsilon_0, t)$ denotes the conditional probability of finding the system in state ϵ at time t if it was in state ϵ_0 at $t = 0$ and the rates $\kappa(\epsilon', \epsilon)$ are those associated with transitions $\epsilon \rightarrow \epsilon'$. Apart from the restriction that the $\kappa(\epsilon', \epsilon)$ have to obey detailed balance and that the form of the population of the states in thermal equilibrium is given by

$$p^{\text{eq}}(\epsilon) = Z^{-1} \eta(\epsilon) e^{-\beta\epsilon}, \quad \text{where } Z = \int d\epsilon p^{\text{eq}}(\epsilon) \quad (2)$$

each specific choice for these transition rates defines a certain model.

In all following calculations we use two models for the $\kappa(\epsilon', \epsilon)$ differing mainly in the connectivity of the states. In both models we assume a common activation energy ϵ_A for the escape out of the initial state ϵ . One scenario we consider is a *globally connected model* (GCM) in which each state ϵ' can be reached from the initial state ϵ . The destination states are chosen randomly according to the DOS. The transition rates for this model read

$$\kappa(\epsilon', \epsilon) = \tilde{\kappa}_\infty \eta(\epsilon') e^{-\beta(\epsilon_A - \epsilon)} = \kappa_\infty \eta(\epsilon') e^{\beta\epsilon}. \quad (3)$$

Here β denotes the inverse temperature and we have absorbed the common activation term $e^{-\beta\epsilon_A}$ in the attempt frequency κ_∞ . With the additional assumption of a Gaussian DOS this model is equivalent to the one used by Dyre [9] and corresponds to a random energy model [39] with a kinetics as studied by Shakhnovich and Gutin [40]. A slightly different form than Eq. (3) was used in a model by Brawer [8].

The other case to be considered is a *locally connected model* (LCM) where starting from a given state ϵ only states of very similar ϵ' can be reached. In this case the master equation (1) is reduced to a Fokker-Planck equation of the form

$$\begin{aligned} \dot{G}(\epsilon, \epsilon_0, t) &= \frac{\partial}{\partial \epsilon} [D(\epsilon)(\beta \partial U(\epsilon)/\partial \epsilon)G(\epsilon, \epsilon_0, t)] \\ &\quad + \frac{\partial^2}{\partial \epsilon^2} [D(\epsilon)G(\epsilon, \epsilon_0, t)], \end{aligned} \quad (4)$$

where we choose

$$D(\epsilon) := \kappa_\infty e^{\beta \epsilon} \quad \text{and} \quad U(\epsilon) := -\beta^{-1} \ln[\eta(\epsilon)]. \quad (5)$$

In this form it is easily verified that the equilibrium solution is given by Eq. (2). In a discrete form this model is similar to the one employed recently to model the dynamics in a solvable glassy system [41].

The reason that we use two quite different scenarios in our calculations is simply to demonstrate that different choices for the transition rates lead to results that differ only quantitatively from each other, the main features being very similar independent of the underlying model. Additionally, we restrict ourselves to the choice of a Gaussian DOS $\eta(\epsilon)$. This means that the mean relaxation times will have a Ferry-like temperature dependence $\propto \exp(T_0/T)^2$ [42]. Other choices can lead to different curvatures of the mean relaxation times as a function of temperature [11]. The use of a Gaussian DOS allows an immediate interpretation of the width of the distribution of the equilibrium populations as being proportional to inverse temperature. This is because Eq. (2) now reads

$$p_G^{\text{eq}}(\epsilon) = \frac{1}{\sqrt{2\pi\sigma}} e^{-(\epsilon - \bar{\epsilon})^2/(2\sigma^2)}, \quad \bar{\epsilon} = -\sigma^2\beta. \quad (6)$$

In the following calculations we give the free-energy variables ϵ as well as the width σ in units of temperature and set $\beta = 1$.

The model we use for both rotational as well as translational motions relies on the assumption that the underlying dynamics is governed by thermally activated transitions in the energy landscape described above. Only if a transition $\epsilon \rightarrow \epsilon'$ occurs are the orientation Ω and the position \mathbf{r} of a tagged molecule allowed to change. One consequence of this assumption is that the stochastic processes $\Omega(t)$ and $\mathbf{r}(t)$ are not Markovian. However, the two-dimensional stochastic processes $[\epsilon(t), \Omega(t)]$ and $[\epsilon(t), \mathbf{r}(t)]$ are examples of so-called composite Markov processes [2].

We model the changes in Ω and \mathbf{r} by angular and translational jumps, respectively, and then calculate the relevant correlation functions as observed in different types of experiments.

To start with let us recall the treatment of molecular reorientations as introduced in I. The transition rates $\kappa(\epsilon, \epsilon')$ determine the changes in molecular orientation Ω . These changes are modeled by angular jumps via an angle θ . The conditional probability for the composite Markov process $[\epsilon(t), \Omega(t)]$ obeys a master equation of the form

$$\begin{aligned} \dot{G}(\{\epsilon, \Omega\}, \{\epsilon_0, \Omega_0\}, t) &= \int d\epsilon' \int d\Omega' W_R(\{\epsilon, \Omega\}|\{\epsilon', \Omega'\}) \\ &\quad \times G(\{\epsilon', \Omega'\}, \{\epsilon_0, \Omega_0\}, t). \end{aligned} \quad (7)$$

Explicit expressions for the transition rates $W_R(\{\epsilon, \Omega\}|\{\epsilon', \Omega'\})$ are given in I. A solution of Eq. (7) is achieved via an expansion in terms of Wigner rotation matrices [43]

$$\begin{aligned} G(\{\epsilon, \Omega\}, \{\epsilon_0, \Omega_0\}, t) \\ = \sum_{l, m, n} \frac{2l+1}{8\pi^2} G_l(\epsilon, \epsilon_0, t) D_{mn}^l(\Omega) D_{mn}^l(\Omega_0)^* \end{aligned}$$

and subsequent solution of the following integrodifferential equations:

$$\begin{aligned} \dot{G}_l(\epsilon, \epsilon_0, t) &= \int d\epsilon' \Pi_l(\epsilon, \epsilon') G_l(\epsilon', \epsilon_0, t), \quad \text{with} \\ \Pi_l(\epsilon, \epsilon') &= - \int d\epsilon'' \kappa(\epsilon'', \epsilon) \delta(\epsilon - \epsilon') \\ &\quad + P(\cos(\theta)) \kappa(\epsilon, \epsilon') [1 - \delta(\epsilon - \epsilon')]. \end{aligned} \quad (8)$$

Here $P_l(\cos(\theta))$ denotes a Legendre polynomial of rank l . If random reorientational jumps are assumed, one has to replace $P_l(\cos(\theta))$ by $\delta_{l,0}$ [1]. Note that the model of small step angular diffusion is obtained in the limit $\theta \rightarrow 0$. From the structure of the matrix $\Pi_l(\epsilon, \epsilon')$ the model assumption that an angular jump occurs only together with an $\epsilon \rightarrow \epsilon'$ transition is immediately evident. The rotational correlation functions for the l th rank Legendre polynomials are given by

$$\begin{aligned} g_l(t) &= \frac{\langle P_l(\Omega(t)) P_l(\Omega_0(0)) \rangle}{\langle P_l(\Omega(0)) P_l(\Omega_0(0)) \rangle} \\ &= \int d\epsilon \int d\epsilon_0 p^{\text{eq}}(\epsilon_0) G_l(\epsilon, \epsilon_0, t). \end{aligned} \quad (9)$$

These functions are given as inhomogeneous superpositions of exponential decays with apparent reorientation rates determined by the eigenvalues of the matrices $\Pi_l(\epsilon, \epsilon')$.

In order to describe the translational motion of the molecules we proceed in exactly the same manner as in the rotational case. We assume that with each transition among the metastable states associated with free-energy minima ϵ there is an associated transition $\mathbf{r} \rightarrow \mathbf{r}'$. The dynamics of the composite Markov process $[\epsilon(t), \mathbf{r}(t)]$ is then governed by the master equation

$$\begin{aligned} \dot{G}(\{\epsilon, \mathbf{r}\}, \{\epsilon_0, \mathbf{r}_0\}, t) \\ = \int d\epsilon' \int d\mathbf{r}' W_T(\{\epsilon, \mathbf{r}\}|\{\epsilon', \mathbf{r}'\}) G(\{\epsilon', \mathbf{r}'\}, \\ \times \{\epsilon_0, \mathbf{r}_0\}, t), \end{aligned} \quad (10)$$

which is completely analogous to Eq. (7). Let us denote the rate for a jump from position \mathbf{r}' in state ϵ' into position \mathbf{r} associated with state ϵ by $\Lambda(\mathbf{r}, \mathbf{r}')$. We then have for the transition matrix:

$$\begin{aligned} W_T(\{\epsilon, \mathbf{r}\}|\{\epsilon', \mathbf{r}'\}) &= - \left\{ \int d\epsilon'' \kappa(\epsilon'', \epsilon) \right\} \delta(\mathbf{r} - \mathbf{r}') \delta(\epsilon - \epsilon') \\ &\quad + \Lambda(\mathbf{r}, \mathbf{r}') [1 - \delta(\epsilon - \epsilon')]. \end{aligned} \quad (11)$$

In principle one would need a detailed model for the transition rates $\Lambda(\mathbf{r}, \mathbf{r}')$. Since we are interested in the description of scattering experiments that employ relatively small momentum transfers, the details of such a model on a microscopic length scale are not of importance. We assume that the displacements proceed via small jumps of length δR . Then the quantity $q\delta R$ gives the experimentally relevant scale, if q denotes the modulus of the scattering vector. Typically, we will be concerned with $q\delta R < 1$. If $q\delta R \ll 1$ holds additionally, then as is shown explicitly further below one is in the regime of Fickian diffusion. For simplicity we consider the following model: We assume that all sites into which a molecule can jump lie on a sphere of radius δR around its initial position, thus enforcing isotropy from the outset. Equivalently one could start from a lattice model and then average over all spatial directions at the end of the calculations [44,45]. Of course in a real liquid there will be a distribution of elementary jump lengths but this complication will not be taken into account here. Additionally, we note that the translational motions associated with transitions among different metastable states ϵ are expected to be highly cooperative. However, here we are mainly concerned with tagged particle motion and thus also neglect this further complexity of the problem in the following considerations.

Equation (10) is dealt with in the following way. We perform a Fourier transform

$$G_{\mathbf{q}}(\epsilon, \epsilon_0, t) = \frac{1}{(2\pi)^3} \int d\mathbf{r} e^{i\mathbf{q}\cdot\mathbf{r}} G(\{\epsilon, \mathbf{r}\}, \{\epsilon_0, \mathbf{r}_0\}, t) \quad (12)$$

and solve the integrodifferential equations ($q = |\mathbf{q}|$):

$$\dot{G}_{\mathbf{q}}(\epsilon, \epsilon_0, t) = \int d\epsilon' \Pi_{\mathbf{q}}(\epsilon, \epsilon') G_{\mathbf{q}}(\epsilon', \epsilon_0, t). \quad (13)$$

Here we have made use already of isotropy and the matrix $\Pi_{\mathbf{q}}(\epsilon, \epsilon')$ is given by

$$\begin{aligned} \Pi_{\mathbf{q}}(\epsilon, \epsilon') = & - \int d\epsilon'' \kappa(\epsilon'', \epsilon) \delta(\epsilon - \epsilon') \\ & + j_0(q\delta R) \kappa(\epsilon, \epsilon') [1 - \delta(\epsilon - \epsilon')], \end{aligned} \quad (14)$$

with $j_0(x) = \sin(x)/x$ denoting a Bessel function. If we introduce the reduced scattering vector

$$Q = q\delta R \quad (15)$$

it is obvious that $G_{\mathbf{q}}(\epsilon, \epsilon_0, t)$ depends only on Q , that is, $G_{\mathbf{q}}(\epsilon, \epsilon_0, t) \equiv G_Q(\epsilon, \epsilon_0, t)$.

The incoherent intermediate scattering function [45] is now easily evaluated to be given by

$$S(Q, t) = \int d\epsilon \int d\epsilon_0 p^{eq}(\epsilon_0) G_Q(\epsilon, \epsilon_0, t), \quad (16)$$

which for $Q \ll 1$ decays exponentially $\propto \exp(-q^2 D_T t)$ with an *effective diffusion coefficient* D_T . This means that we do not assume Fickian diffusion to hold but *calculate* the effective diffusion constant from our model.

For other choices of the transition rates $\Lambda(\mathbf{r}, \mathbf{r}')$ the Bessel function occurring in Eq. (14) would have to be re-

placed by some other function, which, however, also has to tend towards the limit $1 - \frac{1}{6}(Q)^2$ for $Q \rightarrow 0$ since otherwise there would be no diffusive regime at all.

In all the following numerical calculations we use discrete versions of Eqs. (1) and (4), as discussed in I. The integrals occurring in the master equation (1) are replaced by sums $i = 1 \cdots N$ over discrete values ϵ_i spaced homogeneously with a distance $\Delta = \epsilon_{i+1} - \epsilon_i$ and the transition rates $\kappa(\epsilon, \epsilon')$ are written as $\kappa(\epsilon_i, \epsilon_k)$. Then the Fokker-Planck equation (4) may be viewed as a master equation with transition rates

$$\kappa(\epsilon_k, \epsilon_i) = \kappa_{\infty} e^{\beta\epsilon_i/\Delta^2} \{\eta(\epsilon_k)/\eta(\epsilon_i)\}^{1/2} \delta_{k,i\pm 1},$$

where $\delta_{k,i\pm 1}$ denotes a Kronecker symbol. Analogously, the integrals appearing in Eqs. (8) and (13) are converted to sums.

When comparing the expressions for the rotational correlation function and the scattering functions as well as those for $G_Q(\epsilon, \epsilon_0, t)$ and $G_l(\epsilon, \epsilon_0, t)$ the close interrelations between the latter within the framework of our model become apparent. Nevertheless the characteristic time scales for the decay of the rotational correlation functions on the one hand and for $S(Q, t)$ on the other will turn out to be different when compared as a function of the width of the DOS that is of inverse temperature; see below.

III. ROTATIONAL CORRELATION FUNCTIONS

We first turn to the controversy concerning the magnitude of the jump angles characterizing the reorientational motions of molecules in the supercooled liquid regime. If one considers angular jump models for the rotations [46], the ratio of the correlation times $\langle \tau_n \rangle / \langle \tau_m \rangle$ with $n, m = 1, 2, 3, \dots$ is given by

$$\langle \tau_n \rangle / \langle \tau_m \rangle = \{1 - P_m(\cos(\theta))\} / \{1 - P_n(\cos(\theta))\}. \quad (17)$$

Here, we have defined the correlation time as the time integral of the corresponding rotational correlation function $g_l(t)$:

$$\langle \tau_l \rangle = \int_0^{\infty} dt g_l(t). \quad (18)$$

We note that our model defined via Eq. (8) yields a single exponentially decaying correlation function if we allow only for two values of ϵ with equal weights $p^{eq}(\epsilon_1) = p^{eq}(\epsilon_2) = 1/2$. In this case the correlation time is given by $\tau_1^{-1} = \kappa \{1 - P_l(\cos(\theta))\}$, where $\kappa \equiv \kappa(\epsilon_1, \epsilon_2)$ denotes the transition rate.

In the case of small step rotational diffusion, one has $\langle \tau_1 \rangle / \langle \tau_2 \rangle = 3$ and in the case of random reorientational jump models one finds $\langle \tau_1 \rangle$ to be independent of the rank l and thus $\langle \tau_1 \rangle / \langle \tau_2 \rangle = 1$. It is usually then assumed that values of this ratio in the range of 1–2 indicate the predominance of large angular jumps.

In Fig. 1 different first rank rotational correlation functions $g_1(t)$ calculated using Eq. (9) are shown for transition rates chosen according to the GCM, Eq. (3). The width of the Gaussian DOS is set to $\sigma = 2.0$. Note that this quantity is dimensionless since, as noted below Eq. (6), we have set $\beta = 1$. The different curves correspond to different jump angles

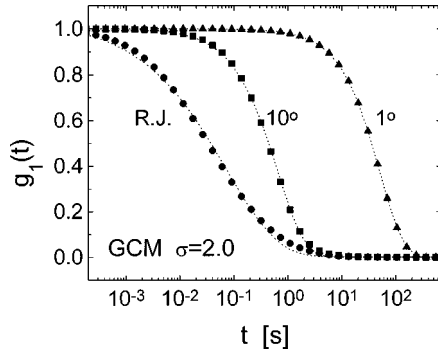


FIG. 1. Rotational correlation function of rank $l=1$, $g_1(t)$ calculated for an angular jump model with various jump angles θ with a kinetics chosen from the GCM, Eq. (3). The calculations were performed for random jumps (RJ) and several jump angles (symbols). The dotted lines represent fits to a Kohlrausch function.

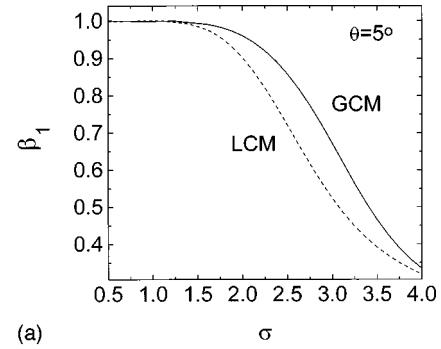
θ . The triangles are for $\theta=1^\circ$, the squares for $\theta=10^\circ$, and the circles are calculated assuming isotropic angular random jumps. It is to be noted that the “angular jump correlation function” defined in Ref. [5] and discussed more extensively in I for all three cases is identical to the function representing the random jump model. This is because the assumption of random angular jumps implies a complete loss of correlation after each jump. This is also the reason for the fact that for the case of random rotational jumps all $g_l(t)$ decay identically, independent of the rank l .

The following two features are evident from Fig. 1: The mean decay time of $g_1(t)$ becomes longer as the angular jump angle θ decreases. Additionally, the stretching of the decay decreases with decreasing θ . Both effects can be understood as consequences of the fact that a smaller angular jump angle leads to a more effective averaging over the $\epsilon \rightarrow \epsilon'$ transitions and thus over the DOS. Consequently the decay of the rotational correlation functions tends to a more exponential form with decreasing jump angle. It should be realized that a complete average over the DOS would yield an exponentially decaying correlation function. The prolongation of the decay is easily understood since for small jump angles more angular jumps are required in order for the rotational correlation function to decay.

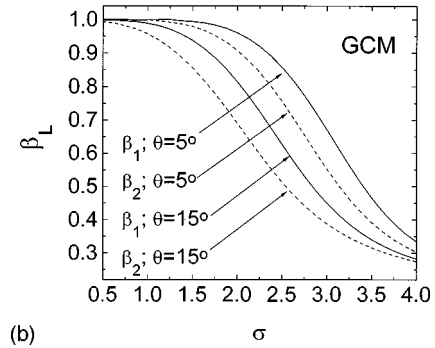
We have calculated the rotational correlation functions $g_l(t)$ for various values of the width σ of the DOS (\propto inverse temperature) and for both the GCM, Eq. (3), and the LCM, Eqs. (4) and (5). For representational convenience these functions are then fitted to a Kohlrausch expression,

$$g_l(t) = e^{-(t/\tau_l)^{\beta_l}}.$$

The dotted lines in Fig. 1 represent such fits. Some results for the stretching parameters β_l from these fits are shown in Fig. 2. We note that the fits to this expression are not always very good, especially for large values of the width σ and large jump angles, where the calculated correlation functions show a prolonged decay as compared to the Kohlrausch law; cf. Fig. 1 and also the discussion in Ref. [5]. Nevertheless, the values of β_l give a good measure for the stretching of the $g_l(t)$. In Fig. 2(a) the exponents β_1 are shown as a function of σ for an angular jump model with $\theta=5^\circ$. It is seen that with increasing width of the DOS the stretching becomes



(a)



(b)

FIG. 2. (a) Stretching parameter β_1 vs the width σ as obtained from fits of rank 1 rotational correlation functions for jump angle $\theta=5^\circ$ for the GCM, Eq. (3) and the LCM, Eq. (4). (b) Stretching parameters β_1 and β_2 vs σ for the GCM.

more pronounced. Furthermore it is evident that within the GCM (full line) a more efficient averaging over the DOS occurs than in the LCM (dashed line) leading to larger values for β_1 . This is to be expected since even though in both cases the same number of transitions are necessary for the rotational correlation function to decay, in the GCM energetically more distinct states ϵ are sampled with a given number of transitions. This leads to a more effective averaging over the DOS.

Figure 2(b) illustrates the difference in the stretching of rotational correlation functions of different rank. The solid lines show β_1 and the dashed lines β_2 . The upper curves are calculated assuming $\theta=5^\circ$ and the lower ones for $\theta=15^\circ$ using the GCM. It is seen that the stretching is more pronounced for $g_2(t)$ at a given width of the DOS than it is for $g_1(t)$. The reason for this is simply that for $l=1$ the orientations have to change roughly by 90° before the rotational correlation function has decayed whereas in the case of $l=2$ about 54° are sufficient for decorrelation. This means that more $\epsilon \rightarrow \epsilon'$ transitions are required for $g_1(t)$ to decay than for $g_2(t)$. This same argument is responsible for the different widths σ at which significant deviations of β_l from unity become obvious for the first time. The number of $\epsilon \rightarrow \epsilon'$ transitions involved in the decay of the rotational correlation functions determines the efficiency of the dynamical averaging over different states ϵ . Thus, β_2 starts to deviate from 1 at a smaller value of σ than β_1 .

We now turn to a comparison of the characteristic decay times of the different $g_l(t)$. We calculated the $\langle \tau_l \rangle$ according to Eq. (18) and plot the results in Fig. 3 for various jump angles. From that plot it is immediately evident that in the case of a sufficiently broad DOS ($\sigma > 2$) the ratio $\langle \tau_1 \rangle / \langle \tau_2 \rangle$

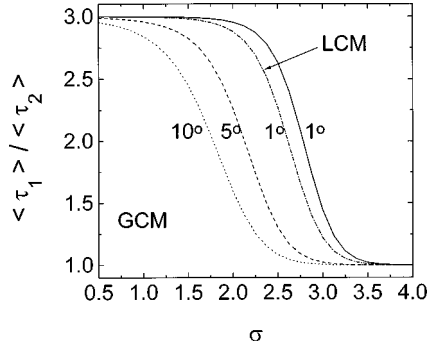


FIG. 3. The ratio of the correlation times as defined in Eq. (18) for $l=1$ and $l=2$, $\langle \tau_1 \rangle / \langle \tau_2 \rangle$ for various jump angles as a function of the width σ of the DOS using the GCM. Also shown is a calculation with the LCM for $\theta=1^\circ$.

does not tell anything about the geometry of the molecular reorientations within the framework of our model. The reason is that there is an intrinsic dynamical averaging that is different for rotational correlation functions of different ranks l . As one can see from Fig. 3 a broader DOS and correspondingly a smaller value of the stretching parameters β_l (cf. Fig. 2) leads to more similar values of $\langle \tau_1 \rangle$ and $\langle \tau_2 \rangle$.

In order to understand this behavior in more detail let us first consider the initial decay rate (at $t \ll \langle \tau_l \rangle$) of the rotational correlation functions as defined by

$$(\tau_l^{\text{in}})^{-1} = -\lim_{t \rightarrow 0} \dot{g}_l(t).$$

As shown in Appendix A from Eq. (9) in conjunction with Eqs. (7) and (8) one finds

$$(\tau_l^{\text{in}})^{-1} = \{1 - P_l(\cos(\theta))\} \int d\epsilon p^{\text{eq}}(\epsilon) \Gamma(\epsilon). \quad (19)$$

Here as in I we have defined the effective decay rate of state ϵ by

$$\Gamma(\epsilon) = \int d\epsilon' \kappa(\epsilon', \epsilon). \quad (20)$$

For large enough temperatures, i.e., widths σ of the DOS that are small enough to allow an effective averaging during the decay of the rotational correlation functions these decay exponentially and the initial decay time coincides with the correlation time, $\tau_l^{\text{in}} = \langle \tau_l \rangle$. Only for this case can Eq. (17) be used to extract a jump angle. Due to the different degrees of dynamical averaging over the DOS inherent in the determination of different $\langle \tau_l \rangle$, as we have seen, Eq. (17) is *not* applicable. However, if this expression is rewritten in terms of the initial decay constants, then one is able to deduce a mean jump angle. This obviously is because the τ_l^{in} are completely independent of any dynamical averaging, since they reflect a short time property ($t \ll \langle \tau_l \rangle$).

From the calculations presented here it is clear that the apparent discrepancy between the NMR results of rather small step angular reorientations on the one hand side and the fact of the already mentioned similarity of $\langle \tau_1 \rangle$ and $\langle \tau_2 \rangle$ can easily be resolved within our model. We note that a *static* distribution of reorientation rates would yield a ratio of

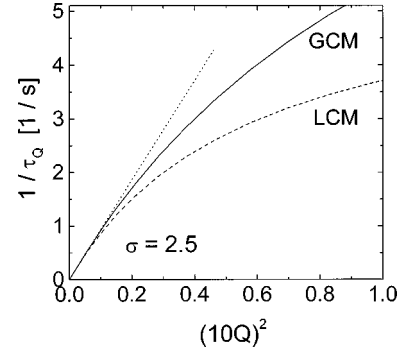


FIG. 4. Inverse decay time of the incoherent intermediate scattering function vs the square of the modulus of the scattering vector as defined in the text. The dotted line represents the diffusive behavior, $1/\tau_Q \propto Q^2$.

$\langle \tau_1 \rangle / \langle \tau_2 \rangle \approx 3$ for all angular jump models we considered as can be seen from the limit of small σ in Fig. 3.

IV. APPARENT TRANSLATIONAL ENHANCEMENT

We have seen above that a model in which a distribution of apparent reorientation rates originates from different transition rates $\kappa(\epsilon, \epsilon')$ yields quite different results for various rotational correlation functions depending on the number of $\epsilon \rightarrow \epsilon'$ transitions necessary for the correlation function under consideration to decay. Since the required average number of transitions is determined by the rank of the rotational correlation function the various jump models considered lead to different decay characteristics. The choice to use a specific experiment sensitive to reorientational motions sets the *rotational* resolution. Using the translational jump model introduced in Sec. II it is the choice of the scattering vector q that tells us about the *spatial* resolution of the experiment and thus about the number of elementary jump events averaged over during the experiment. Thus, conceptually, q in a scattering experiment plays a similar role as the rank l in case of rotational correlation functions.

We proceed in a way that is similar to the computation of the rotational correlation functions in that we calculate the intermediate scattering function according to Eq. (16) as a function of the reduced scattering vector Q and fit the results to a Kohlrausch function:

$$S(Q, t) = e^{-(t/\tau_Q)^{\beta_Q}}.$$

In Fig. 4 we plotted $1/\tau_Q$ versus Q^2 . Only for Q values smaller than roughly 0.1 is $1/\tau_Q$ proportional to Q^2 . This means that we expect Fickian diffusion to be observed on a length scale of approximately ten times the average elementary jump length. In that case the scattering function decays exponentially as $\exp[-(Q/\delta R)^2 D_T t]$ and we identify $1/\tau_Q$ with $(Q/\delta R)^2 D_T$. The width parameter β_Q decreases only slightly below unity for large Q . For $Q=10$ we have $\beta_Q = 0.91$ for the GCM (solid line) and $\beta_Q = 0.86$ for the LCM (dashed line). Of course, outside the diffusive regime ($1/\tau_Q \propto Q^2$) the behavior of $1/\tau_Q$, especially the curvature of $1/\tau_Q$ as a function of Q , strongly depends on the model used for the elementary jump process, cf. the discussion in Sec. II. Also the different efficiency in the dynamical averaging over

the DOS in the GCM and the LCM is clearly evident from Fig. 4. As already pointed out above, we are only interested in the diffusive regime, thus our results will not rely on the jump model.

Within our model the decay constant $1/\tau_Q = (Q/\delta R)^2 D_T$ can be calculated analytically in the limit of small Q values, $\{1 - j_0(Q)\} \approx \frac{1}{6} Q^2$. In close analogy to experimental determinations of the long time diffusion coefficient we compute the long time limit of $S(Q, t)$ for small Q . Since the actual calculation is rather lengthy, we defer it to Appendix B. Here, we only note that the result of this calculation again does not depend on the jump model as its validity is restricted to the diffusive regime. One finds that the decay of $S(Q, t)$ is exponential for long times and the decay time is given by

$$(\tau_Q^{\text{diff}})^{-1} = \frac{1}{6} Q^2 \int d\epsilon p^{\text{eq}}(\epsilon) \Gamma(\epsilon). \quad (21)$$

For later convenience we additionally define the *average rate* $\langle \Gamma \rangle$:

$$\langle \Gamma \rangle := \int d\epsilon p^{\text{eq}}(\epsilon) \Gamma(\epsilon), \quad (22)$$

where the rates $\Gamma(\epsilon)$ are those defined in Eq. (20). With the definition of $\langle \Gamma \rangle$ it is obvious that the translational diffusion coefficient D_T is determined by a *rate average*:

$$D_T = \frac{\delta R^2}{6} \langle \Gamma \rangle. \quad (23)$$

Note that this expression holds only for small Q values.

Alternatively, the decay constant of $S(Q, t)$ as calculated from the initial slope $[-\dot{S}(Q, t \rightarrow 0)]$ analogous to Eq. (19) (cf. Appendix A) yields the same result in the small Q limit. In this calculation the limit $t \rightarrow 0$ is to be understood as $t \ll 1/[(Q/\delta R)^2 D_T]$, since we are solely concerned with the decay of $S(Q, t)$ due to translational motions that are associated with α relaxation and not with processes on shorter time scales. In the case of small scattering vectors $S(Q, t)$ is expected to decay exponentially in the time regime relevant for our considerations and the translational diffusion coefficient is given by Eq. (23). In this case the short time diffusion coefficient and the long time diffusion coefficient coincide as is to be expected for ordinary Fickian diffusion. We mention that relation (23) was checked numerically by comparison with the values for D_T as obtained from fits to $S(Q, t)$.

Next, we compare the values of $\tau_Q = 1/[(Q/\delta R)^2 D_T]$ in the diffusive limit with the rotational correlation times. In Fig. 5(a) the results for the temperature dependence of the correlation times are shown for the GCM. The solid line is τ_Q and the other ones represent $\langle \tau_2 \rangle$ for different angular jump models. It is clear that a strong deviation between the time scales for translation and rotation appears as soon as the width of the DOS exceeds a certain value. This width is the same as the one at which the deviations in $\langle \tau_1 \rangle / \langle \tau_2 \rangle$ from their static values (~ 3) and also the deviations of β_2 from 1 occur. Additionally, it is seen in Fig. 5(a) that larger angular jump angles θ lead to a larger discrepancy between the rotational and the translational correlation times. This is easily

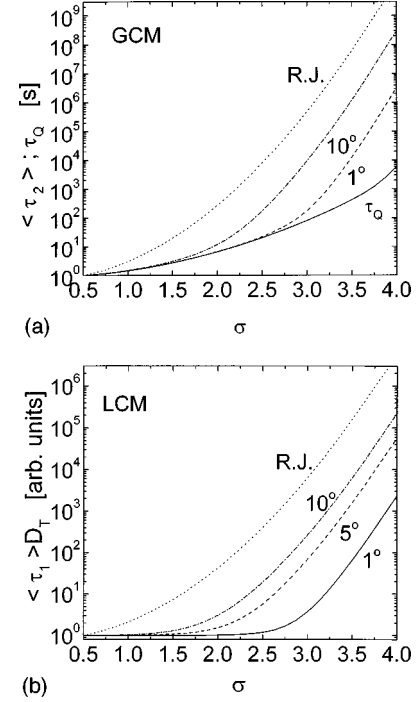


FIG. 5. (a) Rotational correlation times of the second rank rotational correlation function $\langle \tau_2 \rangle$ and the decay time τ_Q of $S(Q, t)$ in the diffusive regime ($Q \leq 0.001$) vs σ for the GCM using different jump angles θ . The dotted line was calculated assuming isotropic random angular jumps. Note that $\langle \tau_{\text{RJ}} \rangle$ is independent of l . All correlation times are scaled to unity for $\sigma = 0$. (b) The product of the translational diffusion coefficient and the rank 1 rotational correlation times for various jump angles using the LCM vs σ . The products are scaled to unity at $\sigma = 0$.

understood because of the different number of $\epsilon \rightarrow \epsilon'$ transitions necessary for the rotational correlation function to decay and the associated different averaging over the DOS, as already discussed in connection with the rotational correlation times. As in all cases discussed before there are only slight quantitative differences when the LCM and the GCM are compared.

The dotted curve in Fig. 5(a) has been calculated assuming random angular jumps. That means that each reorientational jump leads to a complete decorrelation of molecular orientation. Therefore, this is the model that produces the maximum difference between rotation and translation, since in this model no averaging over the different states ϵ occurs in the case of the rotational correlation function. Since the Legendre polynomials occurring in Eq. (8) are replaced by $\delta_{l,0}$ in this case, we can calculate the correlation times $\langle \tau_l \rangle$ analytically from Eq. (8), yielding

$$g_l^{\text{RJ}} = \int d\epsilon p^{\text{eq}}(\epsilon) e^{-\Gamma(\epsilon)t} \quad \text{for } l \neq 0, \quad (24)$$

where the superscript RJ stands for random reorientational jumps. Consequently we have

$$\langle \tau_l^{\text{RJ}} \rangle = \int d\epsilon p^{\text{eq}}(\epsilon) \frac{1}{\Gamma(\epsilon)} \equiv \langle \Gamma^{-1} \rangle. \quad (25)$$

Therefore, the correlation time is just given by the average of the *inverse* decay rates. For finite angular jumps, the correlation times are still given by *time averages* instead of *rate averages* but these times are determined by the eigenvalues of the corresponding matrices $\Pi_l(\epsilon, \epsilon')$ in Eq. (8). Since these eigenvalues determine the effective rotation rates for the considered angular jump model, $\langle \tau_l \rangle$ is given as an average over the effective distribution of apparent rotational correlation times.

Figure 5(b) shows products $\langle \tau_l \rangle D_T$ for the LCM as calculated for various angular jump models versus the width of the DOS. If the Stokes-Einstein and Debye relations would hold, these products should be constant. There is, however, a remarkable increase of the rotational correlation times as compared to the translational diffusion coefficient. According to what we discussed above there are two partly competing effects. The main effect is that the translational diffusion coefficient D_T is determined by the average decay rate $\langle \Gamma \rangle$ whereas the rotational correlation times are given as time averages. The maximum apparent translational enhancement is found for random reorientational jumps and in this case one has within our model

$$D_T \langle \tau_l^{\text{RJ}} \rangle = \frac{\delta R^2}{6} \langle \Gamma \rangle \langle \Gamma^{-1} \rangle. \quad (26)$$

We note that the different averages inherent in the definition of the translational diffusion coefficient and the rotational correlation times have been used as a possible explanation of the apparent translational enhancement quite some time ago [47]. These different averages also have been assumed to be responsible for the apparent translational enhancement in all previous models known to us [30–32]. However, in all these models it was assumed that the Stokes-Einstein and Debye relations hold locally and that the averages performed are averages over distributions of local rotational correlation times and local translational diffusion coefficients, respectively. In our present model we do not assume local correlation times or even diffusion coefficients, but the different averaging originates from different weights of the transition rates $\kappa(\epsilon, \epsilon')$ in the free-energy landscape.

There is, however, another competing effect, which has not to our knowledge been considered earlier and is a direct consequence of the model presented here. If small angular jumps are used to model the rotational motion of the molecules, the maximum apparent translational enhancement, Eq. (26), is diminished due to the dynamical averaging over the $\epsilon \rightarrow \epsilon'$ transitions performed inherently when considering rotational correlation functions of any rank l . The limit that is to be considered in case of exponentially decaying rotational correlation functions is given by

$$D_T \tau_l^{\text{in}} = \frac{\delta R^2}{6} \{1 - P_l(\cos(\theta))\}^{-1}, \quad (27)$$

where τ_l^{in} is defined in Eq. (19) and is determined by the average decay rate $\langle \Gamma \rangle$ just as the translational diffusion coefficient.

V. DISCUSSION

In the last two sections we showed that the model introduced in I can be used for a coherent description of both the translational and the rotational motions of molecules in supercooled liquids. The central assumption of our model consists in a tight coupling of the respective degrees of freedom to the activated dynamics responsible for the α relaxation.

In the case of rotational correlation functions we saw that the rank l of these functions determines the number of elementary transitions necessary for the correlation function to decay. As a larger number of $\epsilon \rightarrow \epsilon'$ transitions leads to a more effective averaging over the DOS (for given width σ) we find different behaviors of the rotational correlation functions as a function of the rank l and additionally of the mean jump angle. We saw that the ratio of the mean correlation times $\langle \tau_1 \rangle / \langle \tau_2 \rangle$ is almost independent of the magnitude of the jump angles but is determined by the inherent *dynamical* averaging over the DOS. Therefore, this ratio is given by its static value (which is approximately 3 for small jump angles) only for very small widths of the DOS since in that case all rotational correlation functions average effectively over the complete set of metastable states ϵ . This also is reflected in the fact that for these small widths the rotational correlation functions decay nearly exponentially. In the other extreme of large widths the ratio $\langle \tau_1 \rangle / \langle \tau_2 \rangle$ approaches unity independent of the magnitude of the jump angles, since then the different efficiency of the dynamical averaging is determined by the different number of transitions required for the rotational correlation functions to decay, leading to a faster decay of the correlation function of rank $l = 1$.

The consequence of these considerations is that a discrimination of various models of reorientational motion in supercooled liquids is not possible in terms of a comparison of correlation times as obtained from different experimental methods. This is an inherent property of our model. All models in which averages over *static* correlation time distributions are performed yield the static values $\langle \tau_1 \rangle / \langle \tau_2 \rangle$, which correspond to our values in the limit of vanishing σ . However, within the framework of such models the experimental observation of small step reorientations in fragile glass-forming liquids is inconsistent with the other experimental finding that $\langle \tau_1 \rangle \approx \langle \tau_2 \rangle$. The model we propose here, on the other hand, provides a simple explanation of these observations, i.e., we have ratios $\langle \tau_1 \rangle / \langle \tau_2 \rangle$ between 1 and 2 also for models with small angular jumps. Thus our model is able to explain the similarity of the rotational correlation times of different ranks l [18–20] and *simultaneously* the fact that the reorientations proceed via small angular steps, as found in NMR experiments [27–29, 48].

In the case of translational motion, we assumed a simple jump model for the elementary translational steps, which leads to Fickian diffusion on a length scale large compared to the mean jump length δR . We showed that rather large apparent translational enhancements occur as a function of the width of the chosen DOS. Since this width is roughly proportional to inverse temperature that means that we expect an increasing translational enhancement with decreasing temperature in qualitative accord with experiment.

In order to see how useful our model is when trying to estimate parameters that are relevant in the supercooled state,

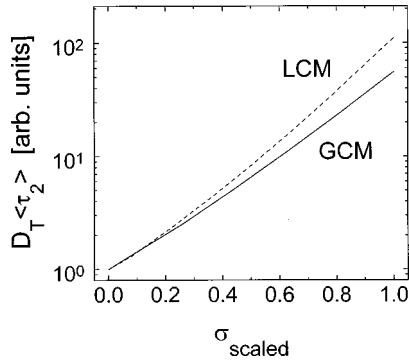


FIG. 6. Product $\langle \tau_2 \rangle D_T$ vs $\sigma_{\text{scaled}} = [\sigma - \sigma(290 \text{ K})] / [\sigma(243 \text{ K}) - \sigma(290 \text{ K})]$ for the GCM as well as for the LCM assuming a jump angle $\theta = 10^\circ$ for the parameters chosen in a way as to represent *o*-TP; see text. In particular this means $\langle \tau_2 \rangle D_T$ has been scaled to unity at a σ that corresponds to $T = 290 \text{ K}$.

we compare some predictions concerning the apparent translational enhancement with experimental results on orthoterphenyl (*o*-TP). We use the values of β_1 from dielectric experiments [49] of Dixon *et al.* [50,51]. From Fig. 2 of Ref. [50] we read off the values of $\beta_1 \sim 0.42$ and 0.53 at approximate temperatures $T \sim T_g = 243 \text{ K}$ and $T \sim 280 \text{ K}$, respectively. A slight extrapolation of the published data yields $\beta_1 \sim 0.59$ at $T = 290 \text{ K}$. This last temperature is the one at which upon cooling the “decoupling” of translational and rotational diffusion becomes significant [26,48]. Since in these experiments the rotational functions of rank $l=2$ (NMR) have been determined, we transform the quoted values of β_1 to the widths σ of our model DOS (cf. Fig. 2) and then calculate the corresponding β_2 from these widths. In doing so we additionally make use of the result that the mean angular jump angle in *o*-TP is approximately $\theta \approx 10^\circ$ [48]. This way we obtain $\sigma(243 \text{ K}) \approx 3.4$, $\beta_2(243 \text{ K}) \approx 0.35$, and $\sigma(290 \text{ K}) \approx 2.7$, $\beta_2(290 \text{ K}) \approx 0.51$ for the GCM. The corresponding values for the LCM are $\sigma(243 \text{ K}) \approx 3.2$, $\beta_2(243 \text{ K}) \approx 0.37$, and $\sigma(290 \text{ K}) \approx 2.3$, $\beta_2(290 \text{ K}) \approx 0.53$. We mention that these values for $\beta_2(243 \text{ K})$ are compatible with those obtained from $^2\text{H-NMR}$ [26,48].

In order to compare the apparent enhancement of translational over rotational diffusion predicted by our model with the experiments on *o*-TP we have plotted the product $\langle \tau_2 \rangle D_T$ as a function of σ in Fig. 6. There we scaled this product to unity at that width σ which corresponds to 290 K . As already mentioned above, the respective values are $\sigma = 2.7$ for the GCM (full line) and $\sigma = 2.3$ for the LCM (dashed line). This means we match the temperature dependences of the rotational and the translational time scales at high temperatures, a procedure that is often adopted when dealing with experimental data. At the corresponding widths $\sigma(243 \text{ K})$, the apparent translational enhancement is about 1.5–2 decades. This value is to be compared with the experimentally found enhancement of roughly 2 decades [26,48]. Thus, the simple estimate presented here is in accord with experiment. However, we think this coincidence should not be overemphasized in view of the crude simplifications inherent in our assumption. The assumption of a single jump angle is of course a serious drawback in a quantitative estimate. It is to be expected that the jump angles are distributed and that the mean jump angle should decrease somewhat when ap-

proaching T_g from above, as has been observed in glycerol [29]. Unfortunately, the temperature dependent variation of the mean jump angle is not available for *o*-TP at present. Another aspect to be borne in mind is the fact that the assumption of a Gaussian DOS has no other meaning than a model parametrization and other choices will lead to quantitatively different results. The overall trends, however, are independent of these model assumptions. Therefore, we think that our model calculations are in qualitative accord with the experimental findings.

From the experimental diffusion coefficients we can give an estimate of the elementary jump length δR in our model. We use the values for the rotational correlation times and diffusion coefficient at $T = 290 \text{ K}$, $\langle \tau_2 \rangle \approx 4 \times 10^{-8} \text{ s}$ and $D_T \approx 2 \times 10^{-13} \text{ m}^2 \text{ s}^{-1}$ from the work of Chang *et al.* [48] and neglect the different dynamical averaging inherent in these values for a moment. Then we can estimate the mean transition rate assuming 10° angular jumps according to $\langle \tau_2 \rangle \sim \langle \kappa \rangle^{-1} \{1 - P_2(\cos(\theta))\}^{-1}$ as $\langle \kappa \rangle \sim 5.6 \times 10^8 \text{ s}^{-1}$. From this value we obtain $\delta R \sim 0.46 \text{ \AA}$ when using $D_T = (\delta R^2/6)\langle \kappa \rangle$. This value roughly corresponds to $\delta R \approx 0.2R_H$, where R_H is the hydrodynamic radius quoted for an *o*-TP molecule [26]. This small value for δR is consistent with the observation of Stillinger and Weber [52] that particles move only about one-tenth of their diameter in a transition between potential energy basins and also the assumptions of Hall and Wolynes [53] in their density functional analysis of the free-energy barriers in hard sphere glasses. Additionally, it is compatible with the observation of Wuttke *et al.* [54] of a crossover to diffusive dynamics in the wave number range of 1 and 0.1 \AA^{-1} in their study of tagged particle motion in glycerol.

It should be noted that the rough estimate of δR based on the relation $\tau_l^{-1} \approx \kappa^{-1} \{1 - P_2(\cos(\theta))\}^{-1}$ [see the discussion below Eq. (18)] is not possible for larger widths σ at lower temperature because of the different dynamical averaging inherent in the determination of the translational diffusion coefficient and the rotational correlation times. However, the conclusion drawn in Ref. [48] that the rms displacement of an *o*-TP molecule during the mean rotational correlation time $\langle \tau_2 \rangle$ is given by $(6D_T\langle \tau_2 \rangle)^{1/2} = 4.7 \text{ nm}$ at $T_g = 243 \text{ K}$ is in full harmony with our model since we are certainly in the diffusive limit at these large displacements. Thus the translational diffusion coefficient is determined by the rate average [cf. Eq. (23)] whereas $\langle \tau_2 \rangle$ represents an average over inverse effective reorientation rates.

Since the mechanism for the apparent translational enhancement is given by the different averages involved in the calculations of the translational diffusion coefficient and the rotational correlation times, we predict that there should be no enhancement if the initial slopes (determined at $t \ll \langle \tau_l \rangle$) of the rotational correlation functions are compared to the translational diffusion coefficient. The product of the initial decay time τ_l^{in} and the translational diffusion coefficient is given by Eq. (27). This ratio is independent of the averages over the decay rates since both quantities are determined solely by $\langle \Gamma \rangle$. On the other hand, within our model a comparison of the initial decay time τ_l^{in} with the translational diffusion coefficient could be used to obtain information about the geometry of the rotational motion of the molecules.

If Eq. (27) is evaluated for a mean reorientational jump angle of $\theta=10^\circ$, one finds a value of $\tau_1^{\text{in}}D_T$ that is larger by a factor of ~ 65 as compared to the corresponding value for random reorientational jumps.

VI. CONCLUSIONS

In this paper we examined the consequences of a very simplistic model for some aspects of α relaxation in supercooled liquids. Since no *ab initio* theoretical description of the dynamical behavior of supercooled liquids exists at present, we use a simple phenomenological model. This model is based on the assumption that below a certain temperature (located in the moderately supercooled regime) ergodicity in the liquid is broken on short time scales and restored on longer time scales by thermally activated transitions among the metastable states. We modeled this activated dynamics in terms of a master equation. Since the modeling of the transitions among the metastable states is not our main concern, we again used very simple kinetic postulates for the transition rates, differing only in their respective connectivity. We used two distinct connectivities in order to show that the details of the model for the transition rates do not change the overall picture, which is in qualitative (or even quantitative) agreement with experiment. The modeling of the rotational and translational degrees of freedom is in the focus of our computations. We assume that only in connection with a transition among the metastable glassy states can the molecules undergo a reorientational as well as a translational elementary process. In the present article we restricted ourselves to dynamics associated with the α process; faster (β) processes are planned to be incorporated into the model in the future.

We modeled both the reorientational as well as the translational motions in terms of finite jump models. That means we assumed that the rotation of molecules proceeds via finite (though essentially small) angular jumps θ and the translational motion via jumps of a mean distance δR . We then showed that concerning the rotational motion such a simple model is able to shed light on some heretofore unresolved aspects with regard to the geometry of the rotations in supercooled liquids. A comparison of rotational correlation times of different ranks l , specifically the ratio $\langle\tau_1\rangle/\langle\tau_2\rangle$, usually is found to be ~ 1 . This is often taken to indicate the predominance of large angular jumps. In fact, it has long been assumed that the angular jump angles are large in fragile supercooled liquids. On the other hand the only method known to us capable of providing detailed information about the jump angles is the so-called stimulated echo and related two-dimensional NMR techniques. In the case of glycerol, toluene, and *o*-TP these experiments clearly show that typical mean elementary reorientation angles are on the order of 10° [26,27,29,48]. We have shown that our model yields ratios of $\langle\tau_1\rangle/\langle\tau_2\rangle\sim 1$ also for such small angles due to the inherent dynamical averaging over the DOS of metastable glassy states. The reason for this finding lies in the fact that for rotational correlation functions of different rank different numbers of transitions are required in order for the correlation function to decay.

When our model is applied to translational motions in the diffusive regime, it is possible to define a translational diffu-

sion coefficient from the decay constant of the incoherent intermediate scattering function. Within the model the translational diffusion coefficient is determined by an average over all transition rates among the metastable states. A comparison of the diffusion coefficient with the corresponding quantity from rotational correlation functions shows a dramatic apparent translational enhancement. This is in qualitative accord with what is observed experimentally. As in earlier models [30–32] the apparent translational enhancement has its origin in the different averages involved in the calculations of the translational diffusion coefficient and the rotational correlation times. However, within the approach developed here it is not necessary to introduce local diffusion coefficients as also assumed, for instance, in Ref. [55]. Consequently, we do not rely on spatial dimensions of, e.g., domains that are large enough to allow Fickian diffusion to be a valid description. Additionally, we were able to show that the apparent translational enhancement should vanish if either the initial decay time of the rotational correlation functions are considered or these correlation functions decay exponentially in time.

We note that we have used the same model in order to describe the results of reduced four-dimensional NMR experiments [1] and were able to show connections between different experimental findings associated with α relaxation in supercooled liquids that had been interpreted as independent features before.

In particular, it is not necessary to introduce a second time scale for environmental fluctuations. In effect, α relaxation is described by a remarkably small number of adjustable parameters in our model. If a Gaussian density of free-energy states $\eta(\epsilon)$ is assumed, its width σ and the attempt frequency κ_∞ [see Eq. (3)] provide the input into Eqs. (1), (8), and (13) for describing rotational and translational molecular motion. The knowledge of the rotational jump angle θ is sufficient for determining the different mean rotational correlation times, stretching parameters, and the amount of apparent translational enhancement as a function of the width σ (see Figs. 2–6).

Concerning heterogeneity, our model has an intrinsic dynamical heterogeneous structure but nothing can be said about spatial aspects of this heterogeneous behavior. In order to obtain such information a more detailed understanding of the activated dynamics in supercooled liquids would be required. We speculate, however, that the free-energy variable ϵ we used to label the metastable glass states should be a function of some coarse grained density. What the appropriate length scale for coarse graining might be is an open question at present in our view.

We close by noting that even though the nature of α relaxation in supercooled liquids is far from being understood theoretically we are nevertheless able to explain several experimental findings with a simple model that is based on the assumption of a strong inherent coupling of the rotational and translational dynamics to the underlying “true” glassy dynamics.

ACKNOWLEDGMENTS

It is a pleasure to thank I. Chang and K. Schug for fruitful discussions. The authors’ work in the subject area was funded by the Deutsche Forschungsgemeinschaft (Grant No. SFB 262).

APPENDIX A: THE INITIAL DECAY RATES

Here, we sketch how the expressions for the initial decay rates $(\tau_l^{\text{in}})^{-1}$, Eq. (19), and $(\tau_Q^{\text{diff}})^{-1}$, Eq. (21), are obtained from the master equations (8) and (13). In order to treat the case of orientational correlation functions $g_l(t)$ and the incoherent scattering function $S(Q,t)$ on the same footing, we introduce a correlation function $\Phi_x(t)$ with $\Phi_x(t)$ representing $g_l(t)$ or $S(Q,t)$, respectively. Thus, x denotes either l in the case of reorientations or Q if translations are considered. In the same way, Eqs. (8) and (13) can be written in a unique way:

$$\dot{G}_x(\epsilon, \epsilon_0, t) = \int d\epsilon' \Pi_x(\epsilon, \epsilon') G_x(\epsilon', \epsilon_0, t) \quad (\text{A1})$$

with

$$\Pi_x(\epsilon, \epsilon') = -\Gamma(\epsilon) \delta(\epsilon - \epsilon') + \psi(x) \kappa(\epsilon, \epsilon') [1 - \delta(\epsilon - \epsilon')]; \quad (\text{A2})$$

cf. Eqs. (8) and (14). Furthermore, we have used the definition Eq. (20) of the effective decay rate $\Gamma(\epsilon)$. In Eq. (A2) $\psi(x)$ stands for the Legendre polynomial $P_l(\cos(\theta))$ in the reorientational case and for the Bessel function $j_0(Q)$ in the case of translational motion. The correlation function is given by

$$\Phi_x(t) = \int d\epsilon \int d\epsilon_0 p^{\text{eq}}(\epsilon_0) G_x(\epsilon, \epsilon_0, t). \quad (\text{A3})$$

We now define an instantaneous decay rate via

$$[\tau_x(t)]^{-1} = -\dot{\Phi}(t)/\Phi(t). \quad (\text{A4})$$

Insertion of Eq. (A3) yields

$$[\tau_x(t)]^{-1} = [1 - \psi(x)] \int d\epsilon_0 p^{\text{eq}}(\epsilon_0) \int d\epsilon \Gamma(\epsilon) G_x(\epsilon, \epsilon_0, t). \quad (\text{A5})$$

In obtaining Eq. (A5) use has been made of the fact that

$$\int d\epsilon \dot{G}_x(\epsilon, \epsilon_0, t) = -[1 - \psi(x)] \int d\epsilon \Gamma(\epsilon) G_x(\epsilon, \epsilon_0, t)$$

as can be shown using Eqs. (A1) and (A2). We point out that the first term stems from the diagonal part of $\Pi_x(\epsilon, \epsilon')$ and the term $\propto \psi(x)$ from the off-diagonal part. The initial decay rate $(\tau_x^{\text{in}})^{-1} = [\tau_x(t=0)]^{-1}$ then reads, using $G_x(\epsilon, \epsilon_0, t=0) = \delta(\epsilon - \epsilon_0)$,

$$(\tau_x^{\text{in}})^{-1} = [1 - \psi(x)] \int d\epsilon p^{\text{eq}}(\epsilon) \Gamma(\epsilon). \quad (\text{A6})$$

This expression is the one given as Eqs. (19) and (21) in the text. It is obvious from this derivation that in the case of single exponentially decaying correlation functions the instantaneous decay rates are time independent and are given by Eq. (A6).

APPENDIX B: THE LONG TIME LIMIT OF $S(Q,t)$ FOR $Q \rightarrow 0$

We will derive the asymptotic long time behavior of the intermediate scattering function $S(Q,t)$, where Q denotes the reduced scattering vector, defined in Eq. (15), in the limit of small Q values, $Q \ll 1$. For simplicity, we use a discrete notation, in which, e.g., Eq. (16) reads

$$S(Q,t) = \sum_{i,j=1}^N p^{\text{eq}}(\epsilon_i) G_Q(\epsilon_i, \epsilon_j, t). \quad (\text{B1})$$

Normalization is such that $\sum_i p^{\text{eq}}(\epsilon_i) = 1$. All results are of course independent of this discretization. In the continuous case all sums occurring in the following are simply to be replaced by the corresponding integrals. We proceed in the following way: We have to solve the master equation, Eq. (13), which reads

$$\dot{G}_Q(\epsilon_i, \epsilon_j, t) = \sum_{k=1}^N \Pi_Q(\epsilon_i, \epsilon_k) G_Q(\epsilon_k, \epsilon_j, t) \quad (\text{B2})$$

with

$$\Pi_Q(\epsilon_i, \epsilon_k) = -\Gamma(\epsilon_i) \delta_{i,k} + j_0(Q) \kappa(\epsilon_i, \epsilon_k) [1 - \delta_{i,k}] \quad (\text{B3})$$

[cf. Eq. (14)] where we have used the definition (20) for the effective decay rate. We now utilize the small Q limit of the Bessel function, $j_0(Q) \approx 1 - \frac{1}{6}Q^2$ in order to define a problem that we can treat in perturbation theory. (Note that in three dimensions every well defined model for diffusion has to show the same limiting behavior as the Bessel function.) We now split the matrix $\Pi_Q(\epsilon_i, \epsilon_k)$ in an obvious way:

$$\Pi_Q(\epsilon_i, \epsilon_k) = \Pi^{(0)}(\epsilon_i, \epsilon_k) + \Pi_Q^{(1)}(\epsilon_i, \epsilon_k). \quad (\text{B4})$$

Here the ‘‘unperturbed’’ problem is defined by

$$\Pi^{(0)}(\epsilon_i, \epsilon_k) = -\Gamma(\epsilon_i) \delta_{i,k} + \kappa(\epsilon_i, \epsilon_k) [1 - \delta_{i,k}] \quad (\text{B5})$$

and is independent of Q . The ‘‘perturbation’’ is given by

$$\Pi_Q^{(1)}(\epsilon_i, \epsilon_k) = -\frac{1}{6}Q^2 \kappa(\epsilon_i, \epsilon_k) [1 - \delta_{i,k}]. \quad (\text{B6})$$

The matrix $\Pi_Q(\epsilon_i, \epsilon_k)$ has the same eigenvalues as the symmetric matrix

$$\tilde{\Pi}_Q(\epsilon_i, \epsilon_k) = [p^{\text{eq}}(\epsilon_i)]^{-1/2} \Pi_Q(\epsilon_i, \epsilon_k) [p^{\text{eq}}(\epsilon_k)]^{1/2}$$

(Ref. [2]). In the limit $Q \rightarrow 0$ Eq. (1) is recovered from Eq. (B2). This particularly means that there is one eigenvector (the largest one), which is zero, $\lambda_0 = 0$. The corresponding eigenvector of the matrix $\tilde{\Pi}^{(0)}(\epsilon_i, \epsilon_k)$ is given by $S_{k,0} = \sqrt{p^{\text{eq}}(\epsilon_k)}$. In terms of the eigenvectors the solution of Eq. (1) after Laplace transformation $f(s) = \int dt e^{-st} f(t)$ reads

$$G(\epsilon_i, \epsilon_j, s) = \sqrt{p^{\text{eq}}(\epsilon_i)/p^{\text{eq}}(\epsilon_j)} \sum_m S_{i,m} S_{j,m} [s - \lambda_m]^{-1}. \quad (\text{B7})$$

This solution allows us to write down the perturbation series with respect to $\Pi_Q^{(1)}(\epsilon_i, \epsilon_k)$:

$$\begin{aligned}
G_Q(\epsilon_i, \epsilon_j, s) &= G(\epsilon_i, \epsilon_j, s) \\
&\quad - \frac{1}{6} Q^2 \sum_{k,l} G(\epsilon_i, \epsilon_k, s) \kappa(\epsilon_k, \epsilon_l) G(\epsilon_l, \epsilon_j, s) \\
&\quad + O(Q^4). \tag{B8}
\end{aligned}$$

Insertion of Eq. (B7) yields

$$\begin{aligned}
G_Q(\epsilon_i, \epsilon_j, s) &= \sqrt{p^{\text{eq}}(\epsilon_i)/p^{\text{eq}}(\epsilon_j)} \left\{ \sum_m S_{i,m} S_{j,m} [s - \lambda_m]^{-1} \right. \\
&\quad - \frac{1}{6} Q^2 \sum_{k,l} \sum_{m,n} S_{i,m} S_{k,m} S_{l,n} S_{j,n} \sqrt{p^{\text{eq}}(\epsilon_l)/p^{\text{eq}}(\epsilon_k)} \\
&\quad \left. \times \kappa(\epsilon_k, \epsilon_l) [s - \lambda_m]^{-1} [s - \lambda_n]^{-1} \right\}. \tag{B9}
\end{aligned}$$

The most important terms in this expression are those with $n=m$. We now neglect the other terms and treat the $n=m$ terms of Eq. (B9) as the first terms of a geometrical series, which we sum. This way we obtain

$$\begin{aligned}
G_Q(\epsilon_i, \epsilon_j, s) &\approx \sqrt{p^{\text{eq}}(\epsilon_i)/p^{\text{eq}}(\epsilon_j)} \\
&\quad \times \sum_m S_{i,m} S_{j,m} [s - \lambda_m - X_m]^{-1}, \tag{B10}
\end{aligned}$$

where we have defined the correction terms:

$$X_m = -\frac{1}{6} Q^2 \sum_{k,l} S_{k,m} S_{l,m} \sqrt{p^{\text{eq}}(\epsilon_l)/p^{\text{eq}}(\epsilon_k)} \kappa(\epsilon_k, \epsilon_l). \tag{B11}$$

Thus, our approximate expression for the intermediate scattering function is

$$S(Q, t) \approx \sum_{i,j} \sqrt{p^{\text{eq}}(\epsilon_i) p^{\text{eq}}(\epsilon_j)} \sum_m S_{i,m} S_{j,m} e^{(\lambda_m + X_m)t}. \tag{B12}$$

From this expression it is seen that in the long time limit only the term with $m=0$ contributes, since all others decay faster due to the negative values of λ_m , $m \neq 0$. (Note that the X_m are negative definite.) Remembering that $S_{k,0} = \sqrt{p^{\text{eq}}(\epsilon_k)}$ and the normalization of the equilibrium populations we find

$$S(Q, t) \sim e^{X_0 t} \quad \text{for } t \rightarrow \infty. \tag{B13}$$

Here, X_0 is given by

$$\begin{aligned}
X_0 &= -\frac{1}{6} Q^2 \sum_l p^{\text{eq}}(\epsilon_l) \sum_k \kappa(\epsilon_k, \epsilon_l) \\
&= -\frac{1}{6} Q^2 \sum_l p^{\text{eq}}(\epsilon_l) \Gamma(\epsilon_l) \equiv -\frac{1}{6} Q^2 \langle \Gamma \rangle, \tag{B14}
\end{aligned}$$

cf. Eq. (22).

Comparison of Eq. (B13) with $S(Q, t) = \exp[-(Q/\delta R)^2 D_T t]$ shows that the long time diffusion coefficient in the limit of small Q is given by Eq. (23).

-
- [1] G. Diezemann, *J. Chem. Phys.* **107**, 1012 (1997).
[2] N. G. van Kampen, *Stochastic Processes in Physics and Chemistry* (North-Holland, Amsterdam, 1981).
[3] A. Heuer, M. Wilhelm, H. Zimmermann, and H. W. Spiess, *Phys. Rev. Lett.* **75**, 2851 (1995).
[4] R. Böhmer, G. Hinze, G. Diezemann, B. Geil, and H. Sillescu, *Europhys. Lett.* **36**, 55 (1996); G. Hinze, R. Böhmer, G. Diezemann, and H. Sillescu, *J. Magn. Res. A* (to be published); R. Böhmer, G. Diezemann, G. Hinze, and H. Sillescu, *J. Chem. Phys.* **108**, 890 (1998).
[5] G. Diezemann, G. Hinze, R. Böhmer, and H. Sillescu, in *Theoretical and Experimental Approaches to Supercooled Liquids: Advances and Novel Applications*, edited by J. Fourkas, D. Kivelson, U. Mohanty, and K. Nelson (ACS Books, Washington, D.C., 1997), Chap. 2.
[6] B. Schiener, R. Böhmer, A. Loidl, and R. V. Chamberlin, *Science* **274**, 752 (1996); B. Schiener, R. V. Chamberlin, G. Diezemann, and R. Böhmer, *J. Chem. Phys.* **107**, 7746 (1997).
[7] M. Goldstein, *J. Chem. Phys.* **51**, 3728 (1969).
[8] S. A. Brawer, *J. Chem. Phys.* **81**, 954 (1984).
[9] J. C. Dyre, *Phys. Rev. Lett.* **58**, 792 (1987); *Phys. Rev. B* **51**, 12 276 (1995).
[10] H. Bässler, *Phys. Rev. Lett.* **58**, 767 (1987).
[11] V. I. Arkhipov and H. Bässler, *J. Phys. Chem.* **98**, 662 (1994).
[12] R. Monasson, *Phys. Rev. Lett.* **75**, 2847 (1993).
[13] C. A. Angell, *J. Res. Natl. Inst. Stand. Technol.* **102**, 171 (1997).
[14] L. Wu, P. R. Dixon, S. R. Nagel, B. D. Williams, and J. P. Carini, *J. Non-Cryst. Solids* **131-133**, 32 (1991).
[15] H.-J. Winkelhahn, Th. K. Servay, and D. Neher, *Ber. Bunsenges. Phys. Chem.* **100**, 123 (1996).
[16] G. Fytas, C. H. Wang, D. Lilge, and T. Dorfmueller, *J. Chem. Phys.* **75**, 4247 (1981).
[17] R. Böhmer, K. L. Ngai, C. A. Angell, and D. J. Plazek, *J. Chem. Phys.* **99**, 4201 (1993).
[18] M. S. Beevers, J. Crossley, D. C. Garrington, and G. Williams, *J. Chem. Soc., Faraday Trans.* **73**, 458 (1977).
[19] D. Kivelson and D. Miles, *J. Chem. Phys.* **88**, 1925 (1988).
[20] D. Kivelson and S. A. Kivelson, *J. Chem. Phys.* **90**, 4464 (1989).
[21] Proceedings of the International Discussion Meeting on Relaxation in Complex Systems, Heraklion, Crete, 1990 [*J. Non-Cryst. Solids* **131-133** (1991)].
[22] H. W. Spiess, in Proceedings of the International Discussion Meeting on Relaxation in Complex Systems (Ref. [21]), p. 378.
[23] G. Williams, in Proceedings of the International Discussion Meeting on Relaxation in Complex Systems (Ref. [21]), p. 379.
[24] G. Williams, *J. Non-Cryst. Solids* **131-133**, 1 (1991).
[25] The question of the angular jump size (of paramagnetic probe molecules) in *o*-TP was also addressed by an electronic spin resonance study. L. Andreozzi, F. Cianflone, C. Donati and D.

- Leporini, J. Phys.: Condens. Matter **8**, 3795 (1996) find that the spin probe performs large angular jumps. Note that from a molecular dynamics simulation, L. J. Lewis and G. Wahnström, Phys. Rev. E **50**, 3865 (1994) also report evidence for large angle motion in the ns-regime.
- [26] F. Fujara, B. Geil, H. Sillescu, and G. Fleischer, Z. Phys. B **88**, 195 (1992).
- [27] G. Hinze, Phys. Rev. E (to be published).
- [28] B. Geil, F. Fujara and H. Sillescu (unpublished).
- [29] R. M. Diehl, F. Fujara, and H. Sillescu, Europhys. Lett. **13**, 357 (1990); R. Böhmer, and G. Hinze (unpublished).
- [30] F. Stillinger and J. A. Hodgdon, Phys. Rev. E **50**, 2064 (1994); H. Sillescu, *ibid.* **53**, 2992 (1996); F. Stillinger and J. A. Hodgdon, *ibid.* **53**, 2995 (1996).
- [31] G. Tarjus and D. Kivelson, J. Chem. Phys. **103**, 3071 (1995).
- [32] I. Chang and H. Sillescu, J. Phys. Chem. **101**, 8794 (1997).
- [33] M. T. Cicerone, P. A. Wagner, and M. D. Ediger, (unpublished).
- [34] W. Götze and L. Sjögren, Rep. Prog. Phys. **55**, 241 (1992).
- [35] F. H. Stillinger, Science **267**, 1935 (1995), and references therein
- [36] D. Thirumalai and R. D. Mountain, Phys. Rev. E **47**, 479 (1993).
- [37] T. R. Kirkpatrick and P. G. Wolynes, Phys. Rev. A **35**, 3072 (1987).
- [38] T. R. Kirkpatrick and D. Thirumalai, J. Phys. A **22**, L149 (1989).
- [39] B. Derrida, Phys. Rev. Lett. **45**, 79 (1980).
- [40] E. I. Shakhnovich and A. M. Gutin, Europhys. Lett. **9**, 569 (1989).
- [41] Th. M. Nieuwenhuizen, Phys. Rev. Lett. **78**, 3491 (1997).
- [42] J. D. Ferry, L. D. Grandine, and E. R. Fitzgerald, J. Appl. Phys. **24**, 911 (1953).
- [43] H. Sillescu, J. Chem. Phys. **104**, 4877 (1996).
- [44] J. W. Haus and K. W. Kehr, Phys. Rep. **150**, 263 (1987).
- [45] M. Bee, *Quasielastic Neutron Scattering* (Adam Hilger, Bristol, 1988).
- [46] J. E. Anderson, Faraday Symp. Chem. Soc. **6**, 82 (1972).
- [47] G. Hinze, Ph.D. thesis, University of Mainz (1993).
- [48] I. Chang, F. Fujara, B. Geil, G. Heuberger, T. Mangel, and H. Sillescu, J. Non-Cryst. Solids **172-174**, 248 (1994).
- [49] In doing so we treat the dielectric response as a single particle correlation function, which may partly be justified if the dipole moments are small or if dilute dipolar probes are used.
- [50] P. K. Dixon, L. Wu, S. R. Nagel, B. D. Williams, and J. P. Carini, Phys. Rev. Lett. **65**, 1108 (1990).
- [51] P. K. Dixon, Phys. Rev. B **42**, 8179 (1990).
- [52] F. H. Stillinger and T. A. Weber, Phys. Rev. A **28**, 2408 (1983).
- [53] R. W. Hall and P. G. Wolynes, J. Chem. Phys. **86**, 2943 (1987).
- [54] J. Wuttke, I. Chang, O. G. Randl, F. Fujara, and W. Petry, Phys. Rev. E **54**, 5364 (1996).
- [55] D. N. Perera and P. Harrowell, J. Chem. Phys. **104**, 2369 (1996).